RECENT QCD RESULTS AT TRISTAN

K.Abe
National Laboratory for High Energy Physics
Tsukuba, Ibaraki 305 Japan

Abstract

Recent QCD results from e^+e^- annihilation experiments at TRISTAN are presented. The R measurements and their implication to $\Lambda_{\overline{MS}}$ is discussed. Multihadron event properties are well described by Lund parton-shower model. The next-to-leading logarithm approximation model also describes event shapes well and in addtion this model allows extraction of the value of $\Lambda_{\overline{MS}}$ which is in good agreement with values determined by other methods. The Bose-Einstein effect is clearly observed at TRISTAN energy.

1. Introduction

TRISTAN e^+e^- storage ring has delivered a total integrated luminosity of 33 pb^{-1} so far in the center-of-mass energy range between 50 and 64 GeV. Three general purpose solenoidal detectors, AMY, TOPAZ, and VENUS have been fully operational during this period. Topics in QCD so far studied include $\Lambda_{\overline{MS}}$ determination, multihadron event properties, difference between quark and gluon jets, gluon-gluon-gluon coupling, and Bose-Einstein correlation. In this talk, I describe a few selected topics from more recent analysis works.

2. R measurements

Figure 1 compares the measured R values at TRISTAN[1,2,3] with the standard model prediction that was calculated by using m_Z=91.1GeV/c^2, $\sin^2\theta_W$=0.23, and $\Lambda_{\overline{MS}}$=300 MeV. The measured values tend to be higher than the prediction in AMY and TOPAZ, whereas the VENUS values are in good agreement.

Fig. 2 shows the R values which were obtained by combining three measurements. A possibility that the R values at TRISTAN energies are higher than the standard model prediction by about 5% cannot be ruled out with the presently available precision. Contributions to the R from quark partons, electroweak effects, and QCD effects are described by

$$R = 3\sum_q (Q_q^2 + \text{electroweak})\left[1 + c_1(\frac{\alpha_s}{\pi}) + c_2(\frac{\alpha_s}{\pi})^2 + c_3(\frac{\alpha_s}{\pi})^3 + \cdots\right] \quad (1)$$

where the strong interaction coupling constant, α_s, is related to the fundamental

QCD cut-off parameter, $\Lambda_{\overline{MS}}$, through a relation

$$\alpha_s(Q^2) = \frac{12\pi}{(32-2N_f)\ln\frac{Q^2}{\Lambda^2_{\overline{MS}}}}\left[1 - \frac{6(153-19N_f)\ln(\ln\frac{Q^2}{\Lambda^2_{\overline{MS}}})}{(32-2N_f)^2\ln\frac{Q^2}{\Lambda^2_{\overline{MS}}}}\right]. \qquad (2)$$

At TRISTAN energies, the electroweak effect is about 25%, and the QCD corrections are in the order of 5%, 0.4%, 1% for 1st, 2nd, and 3rd order terms respectively. It is a well known fact that when all available R data from CESR, DORIS, PEP, PETRA, and TRISTAN are fitted to a parametrization given by Equations (1) and (2), most of the data points of PEP, PETRA, and TRISTAN tend to lie consistently above a fitted curve[1]. When the CESR and DORIS points are excluded from the fit, a fitted value of $\Lambda_{\overline{MS}}$ becomes substantially higher, providing a good agreement between the data and the prediction at PEP and PETRA energies. However, an increase of R in doing this is only 1% at TRISTAN energies and is not enough to explain a possible 5% effect.

3. Multihadron Event Properties

AMY compared their measurements of multihadron event properties with four different multihadron models[4]. These models use either QCD matrix element calculations or QCD cascade approximations at the parton level and let the parton hadronize according to either string or cluster fragmentation. Lund matrix element model(ME)[5] uses the $O(\alpha_s{}^2)$ QCD calculation and the string fragmentation. Lund parton-shower model(PS) is based on the leading-logarithm-approximation(LLA) of the QCD cascade approach and the string fragmentation. Webber model uses the LLA and the cluster fragmentation[6]. Next-to-leading-logarithm parton-shower model(NLL) is an extension of the cascade approach to a higher order[7]. It uses the string fragmentation.

It has been observed that the ME model, which allows only up to four partons, fails to reproduce global features of multihadron event properties at PEP and PETRA energies[4]. The PS model, on the other hand, has been successful in reproducing a wide variety of event shape distributions at lower energies. The Webber model, by adopting a significantly improved handling of the soft-gluon interference, tends to give a better description in the event shape variables in which the string effect plays an important role. Even though both the PS model and the Webber model describe observed event properties well, they do not allow extraction of the value of $\Lambda_{\overline{\rm MS}}$ because of their LLA approach. The NLL model, though based on the cascade approach, allows an unique determination of $\Lambda_{\overline{\rm MS}}$.

Table 1 compares AMY's 22 different event shape variables with these models in terms of χ^2 for overall fits and for several selected variables. The overall χ^2 from a fit to the ME model is 2783 compared with 371 from the PS model. Inadequate description of the data by the ME model persists at TRISTAN energies and they were not included in Table 3. $Q_2 - Q_1$ is a variable which is sensitive to the hard-gluon emission. Here Q_1, Q_2, and Q_3 ($Q_1 \leq Q_2 \leq Q_3$) are magnitudes of the event axis which are defined in terms of the square of the momentum of all tracks in the event. p_T^{out} and aplanarity($=3/2Q_1$) are sensitive to the soft-gluon emission. Rapidity and particle flow are sensitive to the string-effect.

The Lund parton-shower model, without further optimization of the parameters from the values determined at PETRA energy, has a good overall agreement with the data. As can be seen in Figures 3 through 5, the Lund PS model gives better description of $Q_2 - Q_1$, P_T^{out}, and aplanarity compared with the Webber model. However the Webber model is prefered over the Lund PS model in ra-

pidity and particle flow. This is shown in Figure 6 and 7. The NLL model, after their parameters are tuned for the AMY, provides consistently good description in all of these variables.

Table 1. Comparisons of AMY event shape variables with multihadron models.

	Lund PS (default)	Webber (tuned for MarkII)	NLL (tuned for AMY)
$Q_2 - Q_1$	1.7	5.6	2.7
p_T^{out}	5.6	33.3	5.6
aplanarity	2.8	25.5	6.9
rapidity	52.3	25.6	26.6
particle flow	63.5	21.5	24.7
total of 22 variables (194 data points)	371	601	386

4. $\Lambda_{\overline{MS}}$ measurements

Three different methods of extracting the QCD cutoff parameter, $\Lambda_{\overline{MS}}$, were applied on the TRISTAN data. First method uses the R values. The expressions of R and its relation to $\Lambda_{\overline{MS}}$ which weres used in the analysis are given in Equations (1) and (2). Here N_f=5 (N_f=4 below $\sqrt{s}$=11GeV) and $Q^2 = \sqrt{s}$ were used. This method lacks a good sensitivity but has an advantage of not depending on the Monte Carlo hadronization model. AMY fixed the electroweak part with m_Z=91.1GeV/c^2, $\sin^2\theta_W$=0.23, m_t=150GeV/c^2, and m_H=100GeV/c^2. They obtain $\Lambda_{\overline{MS}} = 250^{+150}_{-120}$MeV using the data of AMY in addition to those of

CESR, DORIS, PEP, and PETRA. If the CESR and DORIS points are excluded, the result changes to 380^{+240}_{-190}MeV[1]. In TOPAZ analysis, only m_Z=91.1GeV/c^2 and m_H=100GeV/c^2 are fixed and the rest of the electroweak effect is parameterized as a function of m_t. The result of the two parameter fit, using the data of TOPAZ, PEP, and PETRA, gives $\Lambda_{\overline{MS}} = 354^{+289}_{-194}$MeV[2].

The second method extracts $\Lambda_{\overline{MS}}$ from the asymmetry in the energy-energy correlation. This method has a good sensitivity but a result tends to depend on which hadronization model is used. TOPAZ used the matrix element method by Gottschalk and Shatz and obtained $\Lambda_{\overline{MS}} = 209^{+104}_{-78}$MeV[8].

The third method is based on a multi-jet analysis. Since a main source of three jets events is the qqg production, the three-jet fraction is sensitive to the value of $\Lambda_{\overline{MS}}$. VENUS performed an analysis using the NLL model[9]. Experimentally determined three-jet fractions are compared with the Monte Carlo simulation for different $\Lambda_{\overline{MS}}$ at each y_{cut}. The result is shown in Figure 8. The obtained $\Lambda_{\overline{MS}}$ is reasonably stable except in both very small and very large y_{cut} region where the hadronization model become less reliable. The result is $\Lambda_{\overline{MS}} = 254^{+55}_{-47} \pm 56$MeV at $\sqrt{s}$=58.5GeV. Here the first and second error are statistical and systematic respectively. The multi-jet fractions for both data and a result of the calculation using $\Lambda_{\overline{MS}}$=254MeV are shown as a function of y_{cut} in Figure 9. The calculation are shown for a case in which the hadronization is not included (solid line) and for a case including the hadronozation (dashed line).

5. Bose-Einstein Correlation

AMY has measured the Bose-Einstein correlation using the same-sign $\pi\pi$

to opposite-sign $\pi\pi$ ratio[10]. AMY has no particle identification capability, so that measurements were done in terms of charged track pairs instead of pion pairs. This must be corrected. Further corrections are needed to remove any known effect which generates correlations in same-sign and opposite-sign pion pairs. After all the corrections, the Q^2 dependence of the ratio of same-sign to opposite-sign pions is shown in Figure 10. This distribution is parameterized by

$$R(Q^2) = N_0(1 + \lambda e^{-r_0^2 Q^2})(1 + \gamma Q^2) \quad (3)$$

where N_0 is a normalization constant to take into account the different number of same-sign and opposite-sign pairs, λ and R_0 are the strength and source size in the Bose-Einstein correlation, and the term involving γ is used to take into account long-range correlations that exist such as charge and energy conservation. These parameters were determined to be, $N_0 = 1.021 \pm 0.014, \lambda = 0.603 \pm 0.126, R_0 = 1.182 \pm 0.170\text{fm}, \gamma = -0.041 \pm 0.025(\text{GeV/c})^{-2}$, and $\chi^2/\text{NDF} = 92.5/96$.

The results of λ and R_0 versus center-of-mass energy are shown in Figure 11 together with other measurements in e^+e^- experiments. Also indicated in this figure are the thresholds for charm and bottom production. The λ at TRISTAN energies is consistent with other results obtained above bottom threshold. The source size R_0 measured at TRISTAN seems larger compared with lower energy results which is ≈ 0.8fm and independent of energy. However the discrepancy is only 2.2σ and not statistically significant.

6. Conclusion

The R values measured at TRISTAN is about 5% higher than the standard model prediction that is obtained from $\sin^2\theta_W$=0.23 and now well determined

m_Z=91.1GeV/c^2. This is about 2σ effect. If this is real, it is hard to explain in terms of the QCD correction. The next-to-leading-logarithm approximation of QCD cascade model provides good description of experimental event shape dispributions and, in addition, provides the $\Lambda_{\overline{\rm MS}}$ determination which agrees well with the values determined from other methods. The Bose-Einstein correlation was clearly seen at TRISTAN energy.

References

1) T. Kumita *et al.*(AMY), KEK Preprint 89-188, submitted to Phys.Rev. **D**.
2) I. Adachi *et al.*(TOPAZ), Phys. Lett. **B234**, 525 (1990).
3) K. Abe *et al.*(VENUS), Phys.Lett. **B234**, 382 (1990).
4) Y.C. Li *et al.*(AMY), KEK Preprint 89-149, to be published in Phys. Rev. **D**; H. Sagawa *et al.*(AMY), private communication for the NLL analysis.
5) T. Sjostrand, Comput. Phys. Commun. **39**, 347 (1986).
6) G. Marchesini and B. Webber, Nucl. Phys. **B238**,1(1984); B. Webber, Nucl. Phys. **B238**,492(1984); G. Marchesini and B. Webber, Nucl. Phys. **310**, 461(1988).
7) K. Kato and T. Munehisa, Mod. Phys. Lett. **A1**, 345(1986); K. Kato and T. Munehisa, Phys. Rev. **D36**, 61 (1987); K. Kato and T. Munehisa, Phys. Rev. **D39**, 156 (1989).
8) I. Adachi *et al.*(TOPAZ), Phys. Lett. **B227**, 495 (1989).
9) K.Abe *et al.*(VENUS), KEK Preprint 90-4, to be published in Phys. Lett.**B**.
10) R.C. Walker *et al.*(AMY), private communication.

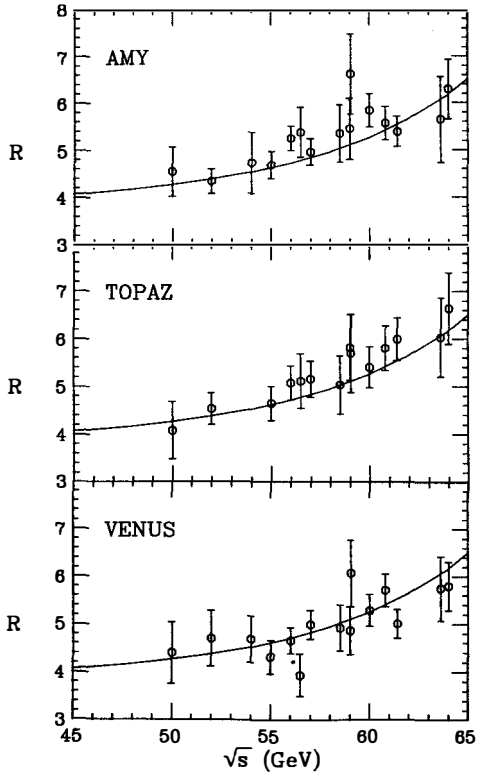

Fig.1 The result of R measurements of AMY(a), TOPAZ(b), and VENUS(c). The standard model prediction that is obtained by using m_Z=91.1GeV/c^2, $\sin^2\theta_W$=0.23, and $\Lambda_{\overline{MS}}$=300MeV is also shown.

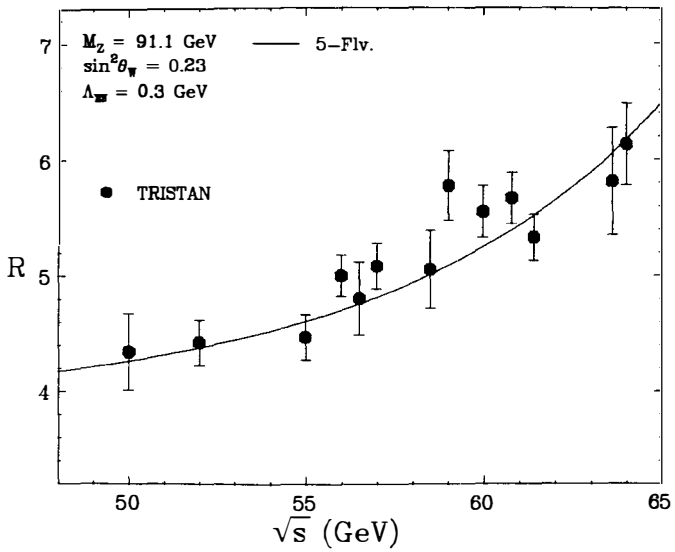

Fig.2 Comparison of the R values, when three TRISTAN measurements are combined, with the standard model.

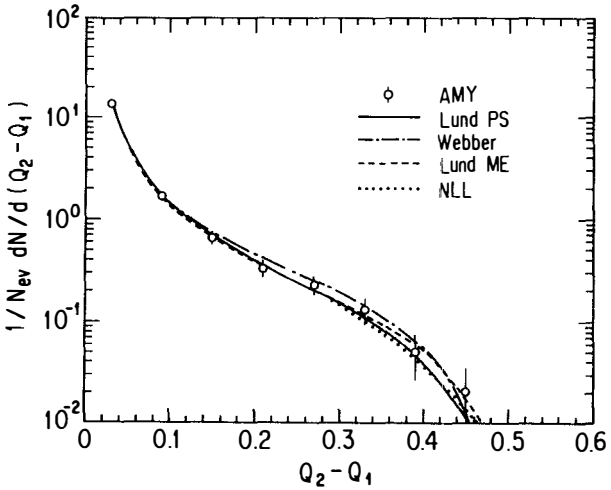

Fig.3 $Q_2 - Q_1$ distribution of AMY multihadron events are compared with predictions of various models.

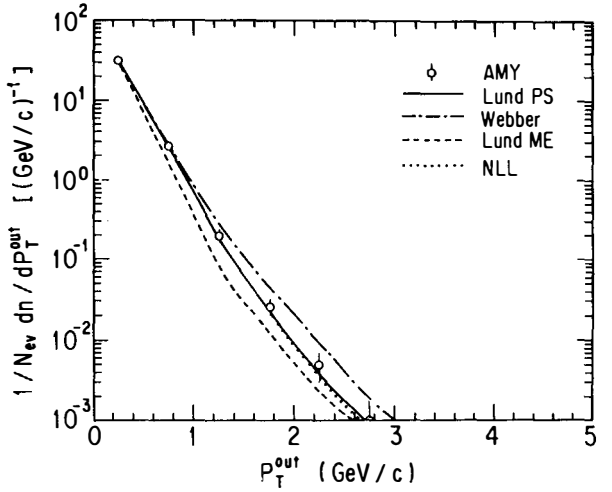

Fig.4 P_T^{out} distribution of AMY data.

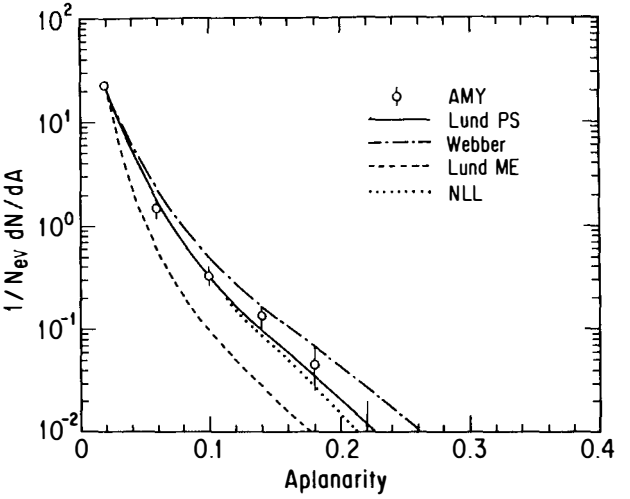

Fig.5 Aplanarity(=$3/2Q_1$) distribution of AMY data.

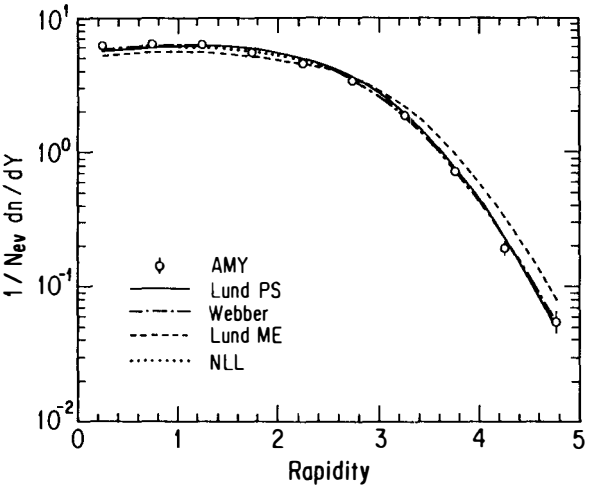

Fig.6 Rapidity distribution of AMY data.

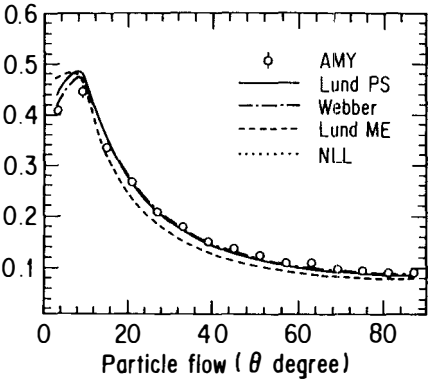

Fig.7 Particle flow distribution of AMY data.

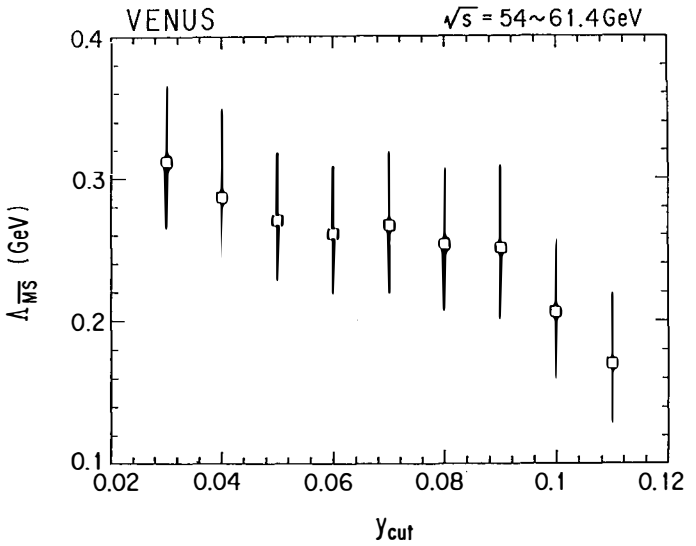

Fig.8 $\Lambda_{\overline{MS}}$ vs y_{cut} in the VENUS analysis.

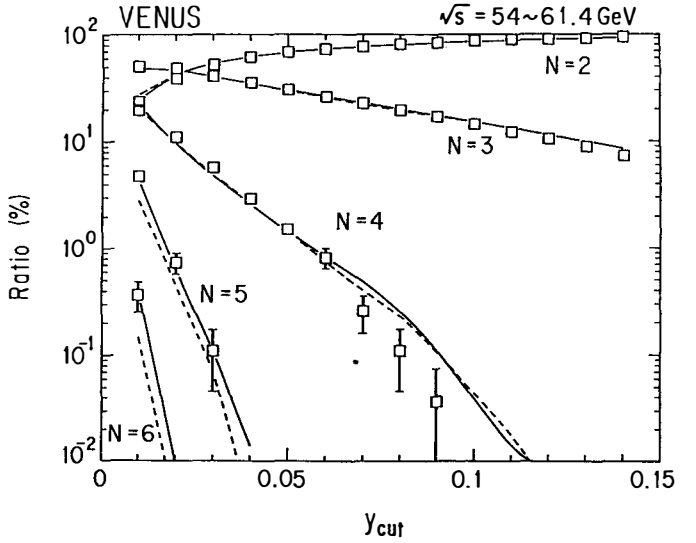

Fig.9 Multijet event ratios vs y_{cut} of VENUS data. Solid (dotted) lines are calculated from the NLL model with (without) hadronization. $\Lambda_{\overline{MS}}$=254MeV is used in the calculation.

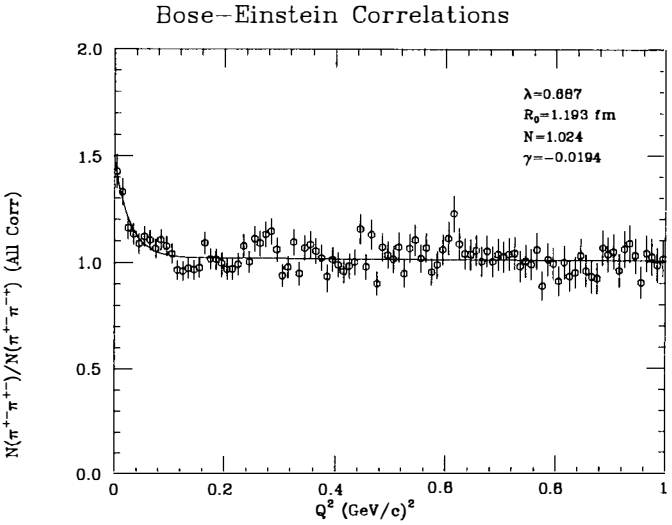

Fig.10 Q^2 distribution of the ratio of the same-sign to opposite-sign pion pairs after all corrections are applied.

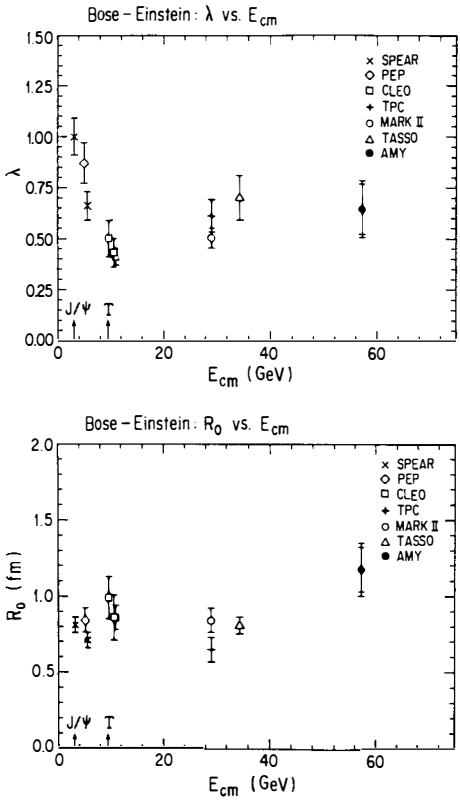

Fig.11 The AMY results of λ and R_0 versus center-of-mass energy are shown together with the results obtained from other e^+e^- experiments.